The Astrophysical Journal, 906:108 (9pp), 2021 January 10 https://doi.org/10.3847/1538-4357/abcb82

From the Fermi Blazar Sequence to the Relation between Fermi Blazars and γ-Ray Narrow-line Seyfert 1 Galaxies

Yongyun Chen[1], Qiusheng Gu[2], Junhui Fan[3], Hongtao Wang[4], Shaojie Qin[5], Nan Ding[6], Xiaoling Yu[2], Xiaotong Guo[2], and Dingrong Xiong[7]
[1] College of Physics and Electronic Engineering, Qujing Normal University, Qujing 655011, People's Republic of China; ynkmcyy@yeah,net
[2] School of Astronomy and Space Science, Nanjing University, Nanjing 210093, People's Republic of China; qsgu@nju.edu.cn
[3] Center for Astrophysics, Guangzhou University, Guangzhou 510006, People's Republic of China
[4] School of science, Langfang Normal University, Langfang 065000, People's Republic of China
[5] Middle School of Tangtang, Town of Xuanwei 655400, People's Republic of China
[6] School of Physical Science and Technology, Kunming University 650214, People's Republic of China
[7] Yunnan Observatories, Chinese Academy of Sciences, Kunming 650011, People's Republic of China
Received 2020 September 1; revised 2020 November 9; accepted 2020 November 16; published 2021 January 14

Abstract

We use the third catalog of blazars detected by Fermi/LAT (3LAC) and γ-ray narrow-line Seyfert 1 Galaxies (γ-NLSy1s) to study the blazar sequence and relationship between them. Our results are as follows. (i) There is a weak anticorrelation between synchrotron peak frequency and peak luminosity for both Fermi blazars and γ-NLSy1s, which supports the blazar sequence. However, after Doppler correction, the inverse correlation disappeared, which suggests that anticorrelation between synchrotron peak frequency and peak luminosity is affected by the beaming effect. (ii) There is a significant anticorrelation between jet kinetic power and synchrotron peak frequency for both Fermi blazars and γ-NLSy1s, which suggests that the γ-NLSy1s could fit well into the original blazar sequence. (iii) According to previous work, the relationship between synchrotron peak frequency and synchrotron curvature can be explained by statistical or stochastic acceleration mechanisms. There are significant correlations between synchrotron peak frequency and synchrotron curvature for whole sample, Fermi blazars and BL Lac objects, respectively. The slopes of the correlation are consistent with statistical acceleration. For FSRQs, LBLs, IBLs, HBLs, and γ-NLS1s, we also find a significant correlation, but in these cases the slopes cannot be explained by previous theoretical models. (iv) The slope of the relation between synchrotron peak frequency and synchrotron curvature in γ-NLS1s is larger than that of FSRQs and BL Lac objects. This result may imply that the cooling dominates over the acceleration process for FSRQs and BL Lac objects, while γ-NLS1s is the opposite.

Unified Astronomy Thesaurus concepts: Active galactic nuclei (16); Blazars (164); Seyfert galaxies (1447)

1. Introduction

Blazars are the most extreme active galactic nuclei (AGN) whose jets are pointing toward us. According to the equivalent width (EW) of the optical emission lines, Blazars are usually divided into two subclasses: flat-spectrum radio quasars (FSRQs) and BL Lac objects. FSRQs have EW > 5 Å, while BL Lac objects are smaller than this value (Urry & Padovani 1995). Later, some authors used other physical parameters to distinguish FSRQs and BL Lac objects. Ghisellini et al. (2011) used the ratio of broad emission line luminosity to Eddington luminosity to divide the FSRQs and BL Lac objects, namely accretion rate. They pointed out that FSRQs have $L_{\rm BLR}/L_{\rm Edd} \geqslant 5 \times 10^{-4}$, while BL Lac objects have $L_{\rm BLR}/L_{\rm Edd} < 5 \times 10^{-4}$. This division between FSRQs and BL Lac objects may imply that they have different accretion regimes (Sbarrato et al. 2014).

Fossati et al. (1998) proposed the so-called "blazar sequence": the synchrotron peak luminosity and Compton dominance are anticorrelated with the synchrotron peak frequency. By fitting the spectral energy distributions (SEDs) of blazars, Ghisellini et al. (1998) confirmed the discovery of Fossati et al. (1998). They suggested that radiative cooling lead to the formation of a blazar sequence. Some authors supported the blazar sequence (Cavaliere & D'Elia 2002; Maraschi & Tavecchio 2003; Maraschi et al. 2008; Ghisellini & Tavecchio 2008; Chen & Bai 2011; Finke 2013; Chen 2014; Xiong et al. 2015). However, some authors opposed this view (Padovani et al. 2003; Nieppola et al. 2006; Padovani 2007; Nieppola et al. 2008; Giommi et al. 2012). The authors mainly considered that the selection effect of the samples lead to the blazar sequence. Nieppola et al. (2008) used a low limit Doppler factor to correct for synchrotron peak frequency and peak frequency luminosity. They found that the anticorrelation between synchrotron peak frequency and peak frequency luminosity disappeared. Meyer et al. (2011) used a large sample of radio-loud AGNs to restudy the blazar sequence. They proposed the blazar envelope: FanaroffRiley (FR) I radio galaxies and most BL Lac objects are "weak-jet" sources, exhibiting radiatively inefficient accretion. However, low synchrotron-peaking (LSP) blazars and FR II radio galaxies are "strong-jet" sources, exhibiting radiative efficient accretion. Finke (2013) found an anticorrelation exists between Compton dominance and the synchrotron peak frequency by using the Second Large-Area Telescope (2LAT) AGN Catalog (Ackermann et al. 2011). Mao et al. (2016) restudied the blazar sequence by using a large sample of blazars from the Roma-BZCAT catalog. They confirmed the original blazar sequence. Ghisellini et al. (2017) used the third Large-Area Telescope AGN Catalog (Ackermann et al. 2015) to revisit the blazar

sequence. They constructed their average spectral energy distribution (SED) by using γ-ray luminosity, and found that the synchrotron peak frequency is anticorrelated with γ-ray luminosity. Their results also support the original blazar sequence.

Besides synchrotron peak frequency and synchrontron peak frequency luminosity, the spectral curvature is also an important physical parameter in the SEDs of blazars. The relationship between the synchrotron peak frequency and the spectral curvature can reflect the acceleration process of particles (Massaro et al. 2004, 2006; Paggi et al. 2009; Tramacere et al. 2009, 2011). However, all these previous studies investigated the relationship between SED peak frequency and its curvature by fitting the SEDs through a log-parabolic function, using observational data with spectral windows close to the synchrotron peak frequency. The choice to use the broadband fit of the synchrotron emission, without a proper physical model, can introduce a significant bias in the estimate of the curvature. Chen (2014) predicted the two particle acceleration mechanisms based on the coefficient of relationship between synchrotron peak frequency and spectral curvature. For stochastic acceleration and statistical acceleration, the slope k ($1/\mathrm{b}_{sy} = k\log\ \nu_p\ +$ c) is 2, 2.5, and 3.33, respectively. They studied this relation by using 43 blazars and found the slope is 2. This result is consistent with stochastic acceleration.

The γ-NLSy1s are the mysterious class of the radio-loud AGN. These γ-NLSy1s show powerful relativistic jets, low black hole mass ($10^6 - 10^8 M_\odot$), and high accretion rate ($0.1 - 1 L_{\rm Edd}$). Some authors thought that their physical properties are similar to blazars. The EW of the broad emission line is larger than 5 Å for all of γ-NLSy1s (Oshlack et al. 2001; Zhou et al. 2007; Yao et al. 2015; Rakshit et al. 2017), which may imply that these γ-NLSy1s can be formally classified as FSRQs. Foschini (2011) studied the characteristics of the jet of blazars and γ-NLSy1s. They found that the jet powers of FSRQs and γ-NLSy1s depend on the black hole mass, while the jet powers of BL Lac objects are dependent on the accretion rate. These results suggested that the accretion disk of FSRQs and γ-NLSy1s are dominated by radiation-pressure, while BL Lac objects are dominated by the gas pressure. Sun et al. (2015) found that the jet properties of γ-NLSy1s resemble that of FSRQs. Paliya et al. (2018) found that the γ-NLSy1s and FSRQs occupy the same region in the Wide-field Infrared Survey Explorer (WISE) color–color diagram. Furthermore, the γ-NLSy1s occupy the low black hole mass end of the FSRQ distribution (Paliya et al. 2018). These γ-NLSy1s may be the counterparts of powerful FSRQs with low black hole mass (Foschini et al. 2015). Chen & Gu (2019) studied the relationship between jet power and accretion disk luminosity in blazars and flat-spectrum radio-loud Narrow-line Seyfert 1 galaxies (FRLNLS1s). They found that the slope of such a relation is similar in FRLNLS1s and blazars. According to the SED modeling, Paliya et al. (2019) found that γ-NLS1s follow the relation between jet power and accretion luminosity seen among blazars. They suggested that the radiation mechanisms of γ-NLS1s are similar to those of blazars.

Many authors have studied the blazar sequence. However, there is no large sample to consider beaming effects when studying the blazar sequence. Thus the blazar sequence has always been controversial. At the same time, there is the question of what the relationship between Fermi blazars and γ-NLS1s is. In this paper, we use a large sample of Fermi blazars and γ-NLSy1s to study the blazar sequence and the relation between Fermi blazars and γ-NLSy1s when considering the beaming effects. The samples are described in Section 2. The results are presented in Section 3. Discussions are in Section 4. Conclusions are in Section 5. The cosmological parameters $H_0 = 70$ kms^{-1} Mpc^{-1}, $\Omega_{\rm m} = 0.3$, and $\Omega_\Lambda = 0.7$ have been adopted in this work.

2. The Sample

2.1. The Sample of Fermi Blazars

We try to collect a larger sample of Fermi blazars with reliable redshift, synchrotron peak frequency, peak frequency luminosity ($L_{\rm zpeak}$), jet power, and Doppler factor. First, we consider the sample of Fan et al. (2016) to get synchrotron peak frequency and peak frequency luminosity. Fan et al. (2016) compiled the multiwavelength data of 1425 Fermi blazars from 3FGL (Acero et al. 2015) to calculate their spectral energy distributions (SEDs). They used a parabolic function to fit the multiwavelength data of 1425 Fermi blazars. The synchrotron peak frequency and peak luminosity were successfully obtained for only 1392 Fermi blazars (461 FSRQs, 620 BL Lac objects, and 311 blazars of uncertain type [BCUs]; 999 sources have known redshifts). Second, we consider the sample of Chen (2018) to get jet power and Doppler factor. According to the leptonic model, Chen (2018) estimated the jet power and Doppler factor of the 1392 Fermi blazars from the catalog of Fan et al. (2016). Finally, we only use the Fermi blazars with reliable redshift and blazars of a certain type. Among the 999 sources with known redshift, 75 were of uncertain type. We therefore get 924 Fermi blazars (461 FSRQ and 463 BL Lac objects, see Table 1).

2.2. The γ-Ray Narrow-line Seyfert 1 Galaxies

We try to collect a large sample of γ-NLS1s with reliable redshift, jet power, and Doppler factor. We consider the sample of Paliya et al. (2019) to get jet power and Doppler factor. Paliya et al. (2019) compiled the largest sample of γ-NLS1s to study their physical properties. They got the jet power and Doppler factor of 16 γ-NLS1s based on the leptonic model. Following the work of Fan et al. (2016), we use a parabolic function to fit the quasi-simultaneous multiwavelength data of 16 γ-NLS1s and get their synchrotron peak frequency and peak frequency luminosity. The fitting formula is as follows

$$\log(\nu F_\nu) = -b(\log\nu - \log\nu_{\rm peak})^2 + \log\nu_{\rm peak} f_{\nu_{\rm p}}, \qquad (1)$$

where b is the spectral curvature, $\log\nu_{\rm peak}$ is the peak frequency, and $\log(\nu_{\rm peak} f_{\nu_{\rm peak}})$ is the peak flux. The sample of γ-NLS1s is shown in Table 2. Figure 1 shows the example of SED of γ-NLS1s.

3. Results

3.1. The Correlation between Synchrotron Peak Frequency and Peak Frequency Luminosity

We study the correlation between synchrotron peak frequency and synchrotron peak frequency luminosity using redshift-corrected values. The synchrotron peak frequency

Table 1
The Physical Parameter of Fermi Blazars

Name (1)	Class (2)	z (3)	δ (4)	$\log P_{\rm jet}$ (5)	$\log \nu_{\rm peak}$ (6)	$\log L_{\rm peak}$ (7)	b (8)
J0001.4+2120	F	1.106	10.7	45.9	16.79	45.70	0.05
J0004.7-4740	F	0.880	12.3	46.2	14.14	46.20	0.12
J0006.4+3825	F	0.229	5.6	45.4	14.03	44.65	0.11
J0008.0+4713	IB	0.280	18.4	46	14.52	44.46	0.12
J0008.6-2340	IB	0.147	51.1	45.8	15.09	44.01	0.10
J0013.9-1853	IB	0.095	29	44.8	14.96	44.37	0.13
J0016.3-0013	F	1.577	6.7	46.4	13.58	45.58	0.09
J0017.6-0512	F	0.227	5	45.1	14.48	44.63	0.11
J0018.4+2947	HB	0.100	14.3	44.9	16.60	43.44	0.06
J0023.5+4454	F	1.062	7.6	46.5	12.78	44.73	0.13
J0024.4+0350	F	0.545	25.5	45.6	13.09	45.37	0.26
J0030.3-4223	F	0.495	6.6	45.8	14.14	45.43	0.12
J0032.3-2852	IB	0.324	71.9	46.5	13.97	44.92	0.15
J0033.6-1921	HB	0.610	12.3	45.1	15.74	45.96	0.11
J0035.2+1513	IB	0.250	27.5	45.5	15.04	44.77	0.12
J0035.9+5949	HB	0.086	14.3	45.6	18.46	44.21	0.04
J0037.9+1239	IB	0.089	25.8	45.6	14.24	43.92	0.14
J0038.0+0012	LB	0.740	14.3	46.4	12.89	45.70	0.25
J0038.0-2501	F	0.498	15.1	45.9	13.26	45.68	0.19

Note. Column (1) gives the 3FGL Name. Column (2) is the class of sources. Column (3) gives the redshift. Column (4) is the Doppler factor. Column (5) is the jet power in units of erg s^{-1}. Column (6) is the synchrotron peak frequency. Column (7) gives the peak frequency luminosity in units of erg s^{-1}. Column (8) is the curvature b. The F is FSRQs; IB is intermediate synchrotron peaked BL Lac objects; HB is high synchrotron peaked BL Lac objects; LB is low synchrotron peaked BL Lac objects. This table is published in its entirety in the electronic edition. A portion is shown here for guidance. The data can be download from http://cdsportal.u-strasbg.fr/my-data/.

Table 2
The Physical Parameter of 16 γ-NLS1s

Name (1)	z (2)	δ (3)	$\log P_{\rm jet}$ (4)	$\log \nu_{\rm peak}$ (5)	$\log L_{\rm peak}$ (6)	b (7)
1H 0323+342	0.061	13.6	45.82	14.98	45.91	0.99
SBS 0846+513	0.584	19.1	46.05	13.65	45.15	0.88
CGRaBS J0932+5306	0.597	14.7	46.54	15.22	44.93	1.25
GB6 J0937+5008	0.275	15.4	46.41	15.04	44.38	1.14
PMN J0948+0022	0.585	15.7	47.11	15.3	45.00	1.19
TXS 0955+326	0.531	12.3	46.68	14.61	45.79	1.63
FBQS J1102+2239	0.453	19	45.86	13.31	44.98	0.57
CGRaBS J1222+0413	0.966	16.5	47.59	14.95	45.89	1.2
SDSS J124634.65 +023809.0	0.362	17.8	45.67	15.67	44.52	1.11
TXS 1419+391	0.49	13.6	46.77	15.15	44.73	1.13
PKS 1502+036	0.407	17.2	46.08	13.34	44.79	0.89
TXS 1518+423	0.484	17.8	46.32	15.9	44.56	1.62
RGB J1644+263	0.145	14.7	45.91	14.56	43.80	0.96
PKS 2004-447	0.24	17.2	45.91	14.67	43.77	1.27
TXS 2116-077	0.26	17.2	45.92	14.46	43.90	1.11
PMN J2118+0013	0.463	14.7	45.99	16.55	44.62	1.35

Note. Column (1) gives the name. Column (2) gives the redshift. Column (3) is the Doppler factor. Column (4) is the jet power in units of erg s^{-1}. Column (5) is the synchrotron peak frequency. Column (6) gives the peak frequency luminosity in units of erg s^{-1}. Column (7) is the curvature b.

luminosity is estimated by using the following formula

$$L_{\rm peak} = 4\pi d_{\rm L}^2 \nu_{\rm peak} F_{\nu,\rm peak}, \quad (2)$$

where d_L is luminosity distance, $d_L\left(z\right) = \frac{c}{H_0}(1+z)\int_0^z [\Omega_\Lambda + \Omega_{\rm m}(1+z')^3]^{-1/2} dz'$ (Venters et al. 2009). The redshift-corrected synchrotron peak frequency is calaulated by using formula

$$\nu_{\rm peak}^{\rm sy} = \nu_{\rm peak}(1+z). \quad (3)$$

Figure 2 shows the relationship between the synchrotron peak frequency luminosity and synchrotron peak frequency. We do not find an "L" or "V" shape in this figure. Fermi blazars and γ-NLS1s are located in the same region. The γ-NLS1s tend to have lower synchrotron peak frequency luminosity than FSRQs. The results of Pearson analysis show that there is a weak negative correlation between $L_{\rm peak}$ and $\nu_{\rm peak}^{\rm sy}$ for the whole sample ($N = 940$, $r = -0.25$, $P = 1.58 \times 10^{-14}$). The scatter of this correlation is $\sigma = 0.86$ dex. The Analysis of Variance (ANOVA) is used to test the results of linear regression, which shows that it is valid for the results of linear regression (value $F = 60.92$, probability $P = 1.58 \times 10^{-14}$). At the same time, we also use Kendall and Spearman tests to analyze these correlations besides Pearson. The results of Kendall ($r = -0.19$, $P = 4.81 \times 10^{-19}$) and Spearman ($r = -0.29$, $P = 2.89 \times 10^{-20}$) tests show that there is also a weak anticorrelation between $L_{\rm peak}$ and $\nu_{\rm peak}^{\rm sy}$ for the whole sample.

Nieppola et al. (2008) proposed that the anticorrelation between the synchrotron peak frequency luminosity and synchrotron peak frequency is affected by the beaming effect. Therefore, we use Doppler factor to correct for synchrotron peak frequency and synchrotron peak frequency luminosity. The Doppler-corrected synchrotron peak frequency is

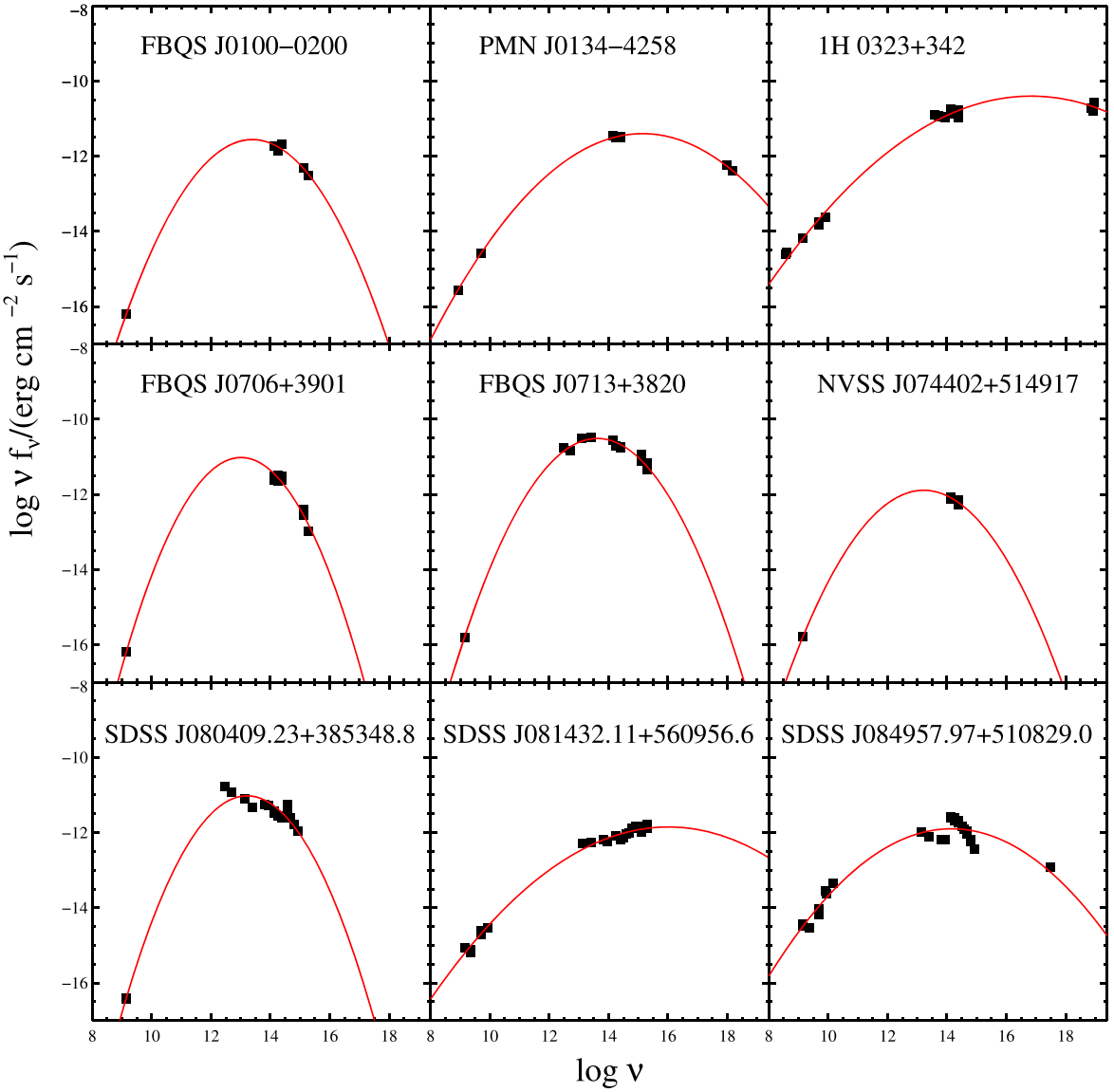

Figure 1. The example of SED fitting of γ-NLS1s.

performed using equation

$$\nu'_{\rm peak} = \frac{\nu^{\rm sy}_{\rm peak}}{\delta}, \quad (4)$$

where $\nu'_{\rm peak}$ indicates the δ-corrected $\nu_{\rm peak}$ in the rest frame. The Doppler-corrected synchrotron peak frequency luminosities are performed using the following formula

$$L'_{\rm peak} = \frac{L_{\rm peak}}{\delta^P}, \quad (5)$$

where $P = 2+\ \alpha$ is a continuous jet and $P = 3+\ \alpha$ is a spherical jet (Urry & Padovani 1995), spectral index $\alpha = 1$.

According to Equations (4) and (5), the Doppler-corrected synchrotron peak frequency luminosity and peak frequency can be obtained (D^2-correction and D^3-correction indicates $P = 2+\alpha$ and $P = 3+\alpha$, respectively). The Doppler-corrected synchrotron peak frequency luminosity versus the Doppler-corrected synchrotron peak frequency is shown in Figure 3. The top panel of Figure 3 ($P = 2+\alpha$) shows that there are significant positive correlations for the whole sample ($r = 0.39$, $P = 8.77 \times 10^{-35}$). The Analysis of Variance (ANOVA) is used to test the results of linear regression, which shows that it is valid for the results of linear regression (value $F = 164.3$, probability $P = 8.77 \times 10^{-35}$). The results of Kendall ($r = 0.25$, $P = 2.42 \times 10^{-30}$) and Spearman ($r = 0.36$, $P = 7.20 \times 10^{-30}$) tests show that there is also a correlation between them for the whole sample. We can find that there are also significant positive correlations between Doppler-corrected synchrotron peak luminosity and the Doppler-corrected synchrotron peak frequency from the bottom of Figure 3 ($P = 3+\alpha$) for the whole sample ($r = 0.46$, $P = 1.83 \times 10^{-50}$). The Analysis of Variance (ANOVA) is used to test the results of linear regression, which shows that it is valid for the results of linear regression (value $F = 252.1$, probability $P = 1.83 \times 10^{-50}$). The results of Kendall ($r = 0.30$, $P = 4.68 \times 10^{-43}$) and Spearman ($r = 0.42$, $P = 5.68 \times 10^{-42}$) tests show that there is also a correlation between them for the whole sample.

At the same time, we should also pay attention to the so-called "bulk Lorentz factor crisis" in particular regarding the HBLs and TeV detected HBLs during Doppler correction. The

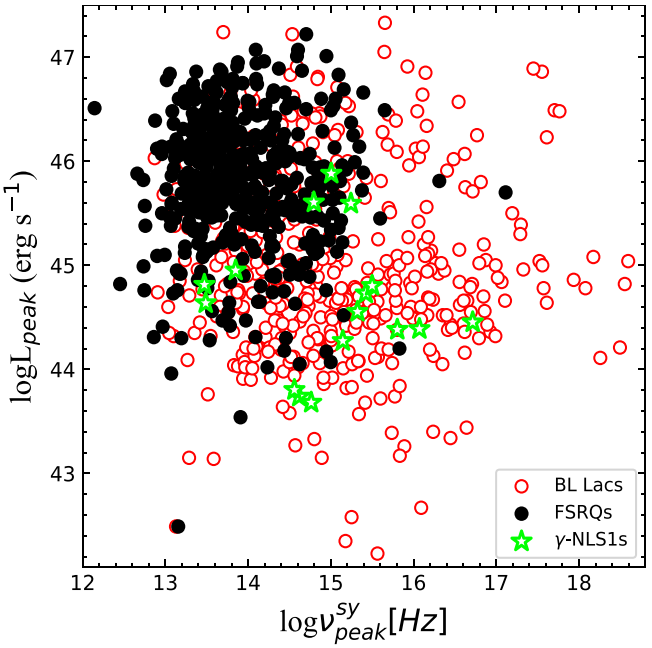

Figure 2. The Synchrotron peak luminosity versus peak frequency for the whole sample. The black filled circles are FSRQs. The red empty circles are BL Lac objects. The green stars are γ-NLS1s.

one-zone synchrotron self-Compton process (SSC) model requires much higher Lorentz/Doppler factor values (Tavecchio et al. 1998; Konopelko et al. 2003; Saugé & Henri 2004; Krawczynski et al. 2001). However, the TeV blazars have no clear superluminal motion, which implies a low Lorentz/Doppler factor in Tev blazars (Piner & Edwarids 2004; Henri & Saugé 2006). In our sample, 43 of the 924 sources are Tev blazars. The 43 TeV blazars include four FSRQs, eight intermediate synchrotron peaked BL Lac objects (IBLs) and 31 high synchrotron peaked BL Lac objects (HBLs). We find that the percentage of TeV blazars is relatively low in our sample, only 4.65%. Therefore, the so-called Lorentz factor crisis does not have a significant impact on our main results when we perform Doppler correction.

3.2. Jet Power versus Synchrotron Peak Frequency

The relation between jet kinetic power and the synchrotron peak frequency is shown in Figure 4. From a Pearson analysis, we find that there is a significant anticorrelation between jet kinetic power and the synchrotron peak frequency for the whole sample ($r = -0.57$, $P = 2.75 \times 10^{-81}$). The Analysis of Variance (ANOVA) is used to test the results of linear regression, which shows that it is valid for the results of linear regression (value $F = 445.9$, probability $P = 2.75 \times 10^{-81}$). The results of Kendall ($r = -0.38$, $P = 2.13 \times 10^{-65}$) and Spearman ($r = -0.54$, $P = 1.04 \times 10^{-71}$) tests show that there is also a significant anticorrelation between them for the whole sample. Furthermore, the γ-NLS1s follow the blazar sequence.

3.3. Synchrotron Peak Frequency versus Synchrotron Curvature

Figure 5 shows the relationship between the synchrotron peak frequency and synchrotron curvature for γ-NLS1s. Here we use $1/b_{sy}$ to represent the synchrotron curvature because it

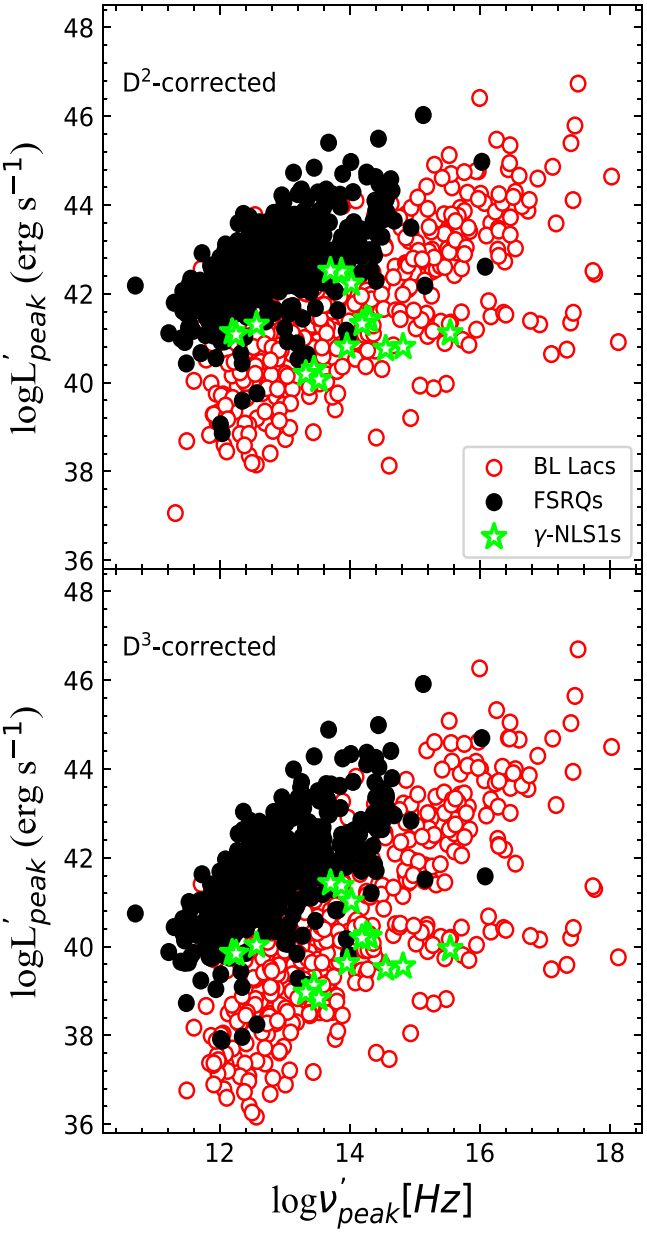

Figure 3. Doppler-corrected synchrotron peak luminosity vs. Doppler-corrected synchrotron peak frequency for Fermi blazars. In the top panel, the data points are D^2-corrected. In the bottom panel, the data points are D^3-corrected.

will be convenient to compare with the theoretical results (see Chen 2014). From a Pearson correlation analysis, there is a significant correlation between synchrotron peak frequency and synchrotron curvature for γ-NLS1s ($r = 0.86$, $p = 1.67 \times 10^{-5}$). The Analysis of Variance (ANOVA) is used to test the results of linear regression, which shows that it is valid for the results of linear regression (value $F = 40.88$, probability $P = 1.67 \times 10^{-5}$). The results of Kendall ($r = 0.62$, $P = 0.0007$) and Spearman ($r = 0.78$, $P = 0.0003$) tests show that there is also a significant correlation between them for the whole sample.

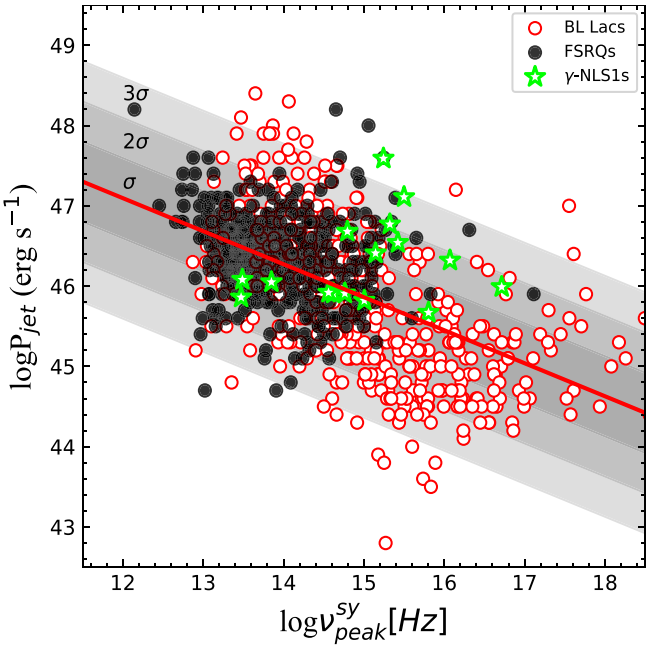

Figure 4. Jet power vs. synchrotron peak frequency for the whole sample. Shaded areas correspond to 1σ, 2σ, and 3σ (vertical) dispersion, where $\sigma = 0.50$ dex. The red line is the least-squares best fit ($\log P_{\rm jet} = -0.41\, log\nu'_{\rm peak} + 52.03$). The meanings of the different symbols are the same as in Figure 2.

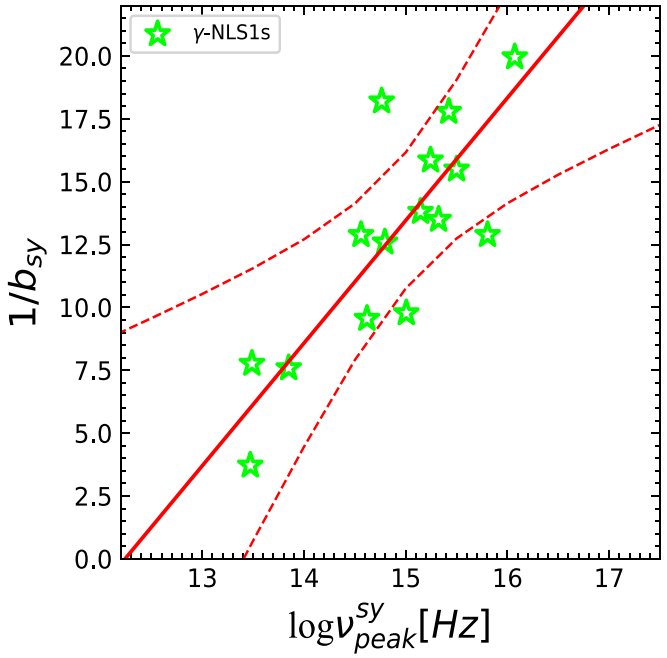

Figure 5. The synchrotron peak frequency versus synchrotron curvature for γ-NLS1s. The red line is the least-squares best fit ($1/b_{\rm sy} = (4.87 \pm 0.76) log\nu^{\rm sy}_{\rm peak} + (-59.79 \pm 11.45)$). The red dashed line is the 3σ confidence level. The meanings of the different symbols are the same as in Figure 2.

4. Discussions

4.1. The Fermi Blazar Sequence

In this paper, we use a large sample of Fermi blazars to study the beaming effects on the blazar sequence. Nieppola et al. (2006) and Meyer et al. (2011) found a "V" or "L" shape in the diagrams of $L_{\rm peak}$ versus $\nu_{\rm peak}$. However, we do not see this shape in Figure 2. Finke (2013) studied blazar sequence by using the 352 second LAT sample. They used the empirical relations of Abdo et al. (2010) to estimate the $\nu_{\rm peak}$ and $L_{\rm peak}$ and found a significant anticorrelation between the $\nu_{\rm peak}$ and $L_{\rm peak}$. By comparing Figure 2 with Figure 2 of Finke (2013), we found that Figure 2 is a bit different from the work of Finke (2013). Our results have a larger dispersion than theirs. These may be due to the different methods. Our sample is larger than theirs. Moreover, we find a weak anticorrelation between synchrotron peak frequency luminosity and the synchrotron peak frequency for the whole sample. These results support the blazar sequence.

The blazar sequence may be affected by the Doppler factor (Nieppola et al. 2008). In the work of Nieppola et al. (2008), the Doppler factor is estimated by using the variability of radio flux, corresponding to a lower limit to the Doppler factor. We use the Doppler factor derived from the synchrotron self-Compton (SSC) emission model (Chen 2018). From Figure 3, we find that after being Doppler-corrected, for all Fermi blazars, the correlations between $L_{\rm peak}$ and $\nu^{\rm sy}_{\rm peak}$ become significant positive correlations, i.e., the anticorrelation between $L_{\rm peak}$ and $\nu^{\rm sy}_{\rm peak}$ disappears, which is consistent with the result of Nieppola et al. (2008). The observational anticorrelation between $L_{\rm peak}$ and $\nu^{\rm sy}_{\rm peak}$ is affected by the Doppler beaming factor.

Synchrotron peak luminosity is strongly affected by the beaming effect. Thus, we study the relationship between intrinsic jet power (jet kinetic power) and the synchrotron peak frequency. We find that there is a significant anticorrelation between $P_{\rm jet}$ and $\nu^{\rm sy}_{\rm peak}$ for Fermi blazars and γ-NLS1s, which supports the blazar sequence, i.e., stronger radiative cooling for higher jet power sources results in smaller energies of the electrons emitting at the peaks.

4.2. The Relation between Fermi Blazars and γ-NLS1s

Paliya et al. (2013) found that the physical properties of γ-NLS1s PKS 1502+036 and PKS 2004-447 are located between FSRQs and BL Lac objects, which implies that theses two sources may belong to the blazar sequence. Foschini (2017) thought that the blazar evolutionary sequence should include NLSy1s. They proposed the evolutionary sequence from NLS1s to BL Lac objects, NLS1s $\rightarrow$ FSRQs $\rightarrow$ BL Lac objects, namely from a small-mass high accreting to a large-mass low accreting black hole. We thus study the relation between Fermi blazars and γ-NLS1s. We fit the SEDs of γ-NLS1s to get the synchrotron peak frequency and peak frequency luminosity. There is an anticorrelation between the synchrotron peak frequency and peak frequency luminosity for both Fermi blazars and γ-NLS1s. The γ-NLS1s follow the synchrotron peak frequency and peak frequency luminosity relation seen among Fermi blazars (Figure 2). At the same time, we also consider the relationship between jet kinetic power and synchrotron peak frequency (Figure 4). There is a significant anticorrelation between jet kinetic power and synchrotron peak frequency for both Fermi blazars and γ-NLS1s. The γ-NLS1s follow the jet kinetic power and synchrotron peak frequency relation seen among Fermi blazars. Our results suggest that these γ-NLS1s could fit well into the traditional blazar sequence. Ghisellini & Tavecchio (2008) proposed that the jet power and the SED of blazars are closely related to the two mian physical parameters of the accretion process, namely

Table 3
The Results of Pearson Correlation Analysis for the Samples

Sample	$1/b_{\rm sy} = A \log \nu^{\rm sy}_{\rm peak} + B$				
	A	B	r	p	F
Whole sample	2.44 ± 0.06	-26.13 ± 0.89	0.79	3.16×10^{-202}	1566
Fermi blazars	2.40 ± 0.06	-25.53 ± 0.88	0.79	4.27×10^{-202}	1580
FSRQs	3.69 ± 0.13	-42.89 ± 1.79	0.80	2.98×10^{-105}	833.5
BL Lac objects	2.56 ± 0.07	-28.75 ± 1.11	0.85	3.84×10^{-132}	1229
LBLs	3.46 ± 0.64	-40.55 ± 8.73	0.51	7.02×10^{-7}	28.96
IBLs	1.67 ± 0.33	-15.72 ± 4.79	0.33	7.12×10^{-7}	26.13
HBLs	3.09 ± 0.18	-37.33 ± 2.89	0.80	2.48×10^{-39}	305.9
γ-NLS1s	4.87 ± 0.76	-59.79 ± 11.45	0.86	1.67×10^{-5}	40.88

Note. The A is slope; B is the intercept; r is correlation coefficient; p is significance level ($p < 0.01$); F is statistical testing of linear regression.

black hole mass and accretion rate. The radiative cooling leads to the observational phenomenon of the blazar sequence (Ghisellini et al. 1998). The FSRQs have high accretion rates, which leads to the fast cooling of relativistic electrons. FSRQs have low synchronous peak frequency and high jet power. However, BL Lac objects have low accretion rates, which leads to the slow cooling of relativistic electrons. BL Lac objects have high synchronous peak frequency and lower jet power. Some works have found that γ-NLS1s have high accretion rate (Foschini 2017; Chen & Gu 2019). The accretion rate of γ-NLS1s is similar to FSRQs, which imply that relativistic electrons of the jet of FSRQs and γ-NLS1s are fast cooling. The γ-NLS1s may belong to the Fermi blazar sequence.

4.3. Particle Acceleration Mechanisms for Fermi Blazars and γ-NLS1s

The correlation between $\log\nu^{\rm sy}_{\rm peak}$ and $1/b_{\rm sy}$ can be explained by two different scenarios, namely the statistical acceleration and the stochastical acceleration mechanisms (Chen 2014). Following the same approach of Chen (2014), i.e., to investigate the particle acceleration. We investigate the relationship between $\log\nu^{\rm sy}_{\rm peak}$ and $1/b_{\rm sy}$ for Fermi blazars and γ-NLS1s. The results are shown in Table 3. We get the relationship between $\log\nu^{\rm sy}_{\rm peak}$ and $1/b_{sy}$ for the whole sample ($N = 940$, $r = 0.79$, $F = 1566$, $P = 3.16 \times 10^{-202}$)

$$1/b_{\rm sy} = (2.44 \pm 0.06) log\nu^{\rm sy}_{\rm peak} + (-26.13 \pm 0.89) \quad (6)$$

and for Fermi blazars ($N = 924$, $r = 0.79$, $F = 1580$, $P = 4.27 \times 10^{-202}$),

$$1/b_{\rm sy} = (2.40 \pm 0.06) log\nu^{\rm sy}_{\rm peak} + (-25.53 \pm 0.88) \quad (7)$$

and for FSRQs ($N = 461$, $r = 0.80$, $F = 833.5$, $P = 2.98 \times 10^{-105}$),

$$1/b_{\rm sy} = (3.69 \pm 0.13) log\nu^{\rm sy}_{\rm peak} + (-42.89 \pm 1.79) \quad (8)$$

and for BL Lac objects ($N = 463$, $r = 0.85$, $F = 1229$, $P = 3.84 \times 10^{-132}$),

$$1/b_{\rm sy} = (2.56 \pm 0.07) log\nu^{\rm sy}_{\rm peak} + (-28.75 \pm 1.11) \quad (9)$$

and for low synchrotron peaked BL Lac objects (LBLs, $N = 83$, $r = 0.51$, $F = 28.96$, $P = 7.02 \times 10^{-7}$),

$$1/b_{\rm sy} = (3.46 \pm 0.64) log\nu^{\rm sy}_{\rm peak} + (-40.55 \pm 8.73) \quad (10)$$

and for intermediate synchrotron peaked BL Lac objects (IBLs, $N = 214$, $F = 26.13$, $r = 0.33$, $P = 7.12 \times 10^{-7}$),

$$1/b_{\rm sy} = (1.67 \pm 0.33) log\nu^{\rm sy}_{\rm peak} + (-15.72 \pm 4.79) \quad (11)$$

and for high synchrotron peaked BL Lac objects (HBLs, $N = 166$, $r = 0.80$, $F = 305.9$, $P = 2.48 \times 10^{-39}$),

$$1/b_{\rm sy} = (3.09 \pm 0.18) log\nu^{\rm sy}_{\rm peak} + (-37.33 \pm 2.89) \quad (12)$$

and for γ-NLS1s ($r = 0.86$, $F = 40.88$, $P = 1.67 \times 10^{-5}$),

$$1/b_{\rm sy} = (4.87 \pm 0.76) log\nu^{\rm sy}_{\rm peak} + (-59.79 \pm 11.45) \quad (13)$$

We find that the slopes of the correlation between synchrotron peak frequency and synchrotron curvature of the whole sample ($k_{\rm whole\ sample} = 2.44 \pm 0.06$), Fermi blazars ($k_{\rm Fermi\ blazars} = 2.40 \pm 0.06$), and BL Lac objects ($k_{\rm BLLacs} = 2.56 \pm 0.07$) are consistent with statistical acceleration for the case of energy-dependent acceleration probability. However, for FSRQs, LBLs, IBLs, HBLs, and γ-NLS1s, the slopes of the correlation are not consistent with any theoretical values ($k = 5/2$, $10/3$, and 2).

Chen (2014) used a sample of 43 blazars to study the correlation between synchrotron peak frequency and synchrotron curvature. They determined that the slope of the correlation was 2.04 ± 0.03, which is consistent with the stochastic acceleration. The sample of Chen (2014) was too small to separate them into FSRQs, BL Lac objects, LBLs, IBLs, and HBLs. Maybe that is why they did not find different slopes between FSRQs, BL Lac objects, LBLs, IBLs, and HBLs. At the same time, our results are different from their results, which may be due to the difference in the number of samples.

The slope of the correlation for FSRQs $k_{\rm FSRQs} = 3.69 \pm 0.13$ is close to $10/3$, which can be explained by statistical particle acceleration for the case of fluctuation of the fractional acceleration gain. Xue et al. (2016) studied the relation between synchrotron peak frequency and synchrotron curvature by using a sample of the second LAT AGN catalog (2LAC). They found that the slope of the correlation for FSRQs is $k_{\rm FSRQs} = 3.69 \pm 0.24$. Our results are consistent with theirs. We find that the slope of the correlation for IBLs $k_{\rm IBLs} = 1.67 \pm 0.33$ is close to 2, which can also be explained by stochastic particle acceleration. Kapanadze et al. (2020) studied the X-ray spectra of BL Lac objects and found the stochastic acceleration in the relativistic jets of BL Lac objects. The slopes of the correlation for LBLs $k_{\rm LBLs} = 3.46 \pm 0.64$

and HBLs $k_{\rm HBLs} = 3.09 \pm 0.18$ are close to 10/3, which can be explained by statistical particle acceleration for the case of fluctuations of the fractional acceleration gain.

The slope of the correlation for γ-NLS1s $k_{\gamma-{\rm NLS1s}} = 4.87 \pm 0.76$ is not close to any theoretical values. Its slope is slightly large than that of FSRQs and BL Lac objects. These results may be explained in the framework of acceleration and cooling processes (Tramacere et al. 2011). In the acceleration process, there is a significant dispersion on the energy gain, leading to a momentum diffusion term, a decreasing curvature (namely increasing of $1/b_{sy}$) leads to a shift of the peak frequency toward higher peak frequency. Hence, the correlation between the peak frequency and curvature is negative. However, the slope of this correlation can change when the cooling dominates over the acceleration process (Tramacere et al. 2011; Kalita et al. 2019). Tramacere et al. (2011) suggested that the magnetic field plays an important role in the evolution of the spectral parameters. They proposed that when the magnetic field is weak, the evolution of the particles around the peak is dominated by the acceleration process, while it is driven by cooling for strong magnetic field. Paliya et al. (2019) found that the average magnetic field derived for γ-NLS1s is relatively lower ($\langle B \rangle = 0.91 \pm 0.33$ G) compared to Fermi blazars (1.83 ± 0.25 G). These results may imply that the cooling dominates over the acceleration process for Fermi blazars, while the acceleration dominates over the cooling process for γ-NLS1s. The slopes of γ-NLS1s, FSRQs, and BL Lac objects seem to form an evolutionary sequence, γ-NLS1s $\rightarrow$ FSRQs $\rightarrow$ BL Lac objects, namely from acceleration (high slope) to cooling process (low slope). Foschini (2017) thought that the evolutionary sequence γ-NLS1s $\rightarrow$ FSRQs $\rightarrow$ BL Lac objects may be the different stages of the cosmological evolution of the same type of source (young $\rightarrow$ adult $\rightarrow$ old). In the early stage of evolution, the acceleration dominates the spectral evolution. At a later stage of evolution, the cooling dominates over the acceleration process (Tramacere et al. 2011). At the same time, we also pay attention to whether our results might have an intrinsic bias, given by the choice to fit the full low-energy bump of the SED.

5. Conclusions

We use a large sample of Fermi blazars and γ-NLS1s to study the Fermi blazar sequence and the relation between them.

1. There is a weak anticorrelation between synchrotron peak frequency luminosity and the synchrotron peak frequency for both Fermi blazars and γ-NLS1s, which supports the blazar sequence.
2. The Doppler-corrected peak frequency luminosity and Doppler-corrected synchrotron peak frequency is positively correlated for the whole sample, which suggests that the relationship between synchrotron peak frequency and synchrotron frequency luminosity is affected by the beaming effect.
3. There is a significant anticorrelation between jet kinetic power and the synchrotron peak frequency for both Fermi blazars and γ-NLS1s, which suggests that the γ-NLS1s could fit well into the traditional blazar sequence.
4. There is a significant correlation between synchrotron peak frequency and synchrotron curvature for the whole sample, Fermi blazars, and BL Lac objects, respectively. The slopes of such a correlation are consistent with statistical acceleration for the case of energy-dependent acceleration probability. For FSRQs, LBLs, IBLs, HBLs, and γ-NLS1s, we also find a significant correlation, but in these cases the slopes cannot be explained by previous theoretical models.
5. The slope of the relation between synchrotron peak frequency and synchrotron curvature in γ-NLS1s is larger than that of FSRQs and BL Lac objects. This result may imply that the cooling dominates over the acceleration process for FSRQs and BL Lac objects, while the acceleration dominates over the cooling process for γ-NLS1s.

We are very grateful to the referee for the very helpful comments and suggestions. This work was support from the research project of Qujing Normal University (2105098001/094). This work is supported by the National Natural Science Foundation of China (NSFC 11733001). This work is supported by the National Key Research and Development Program of China (No. 2017YFA0402703) and the National Natural Science Foundation of China (Grant No. 11733002 and 11773013).

ORCID iDs

Yongyun Chen https://orcid.org/0000-0001-5895-0189
Qiusheng Gu https://orcid.org/0000-0002-3890-3729
Junhui Fan https://orcid.org/0000-0002-5929-0968
Xiaotong Guo https://orcid.org/0000-0002-2338-7709
Dingrong Xiong https://orcid.org/0000-0002-6809-9575

References

Abdo, A. A., Ackermann, M., Agudo, I., et al. 2010, ApJ, 716, 30
Acero, F., Ackermann, M., Ajello3, M., et al. 2015, ApJS, 218, 23
Ackermann, M., Ajello, M., Allafort, A., et al. 2011, ApJ, 743, 171
Ackermann, M., Ajello, M., Atwood, W. B., et al. 2015, ApJ, 810, 14
Cavaliere, A., & D'Elia, V. 2002, ApJ, 571, 226
Chen, L. 2014, ApJ, 788, 179
Chen, L. 2018, ApJS, 235, 39
Chen, L., & Bai, J. M. 2011, ApJ, 735, 108
Chen, Y. Y., & Gu, Q. S. 2019, Ap&SS, 364, 123
Fan, J. H., Yang, J. H., Luo, G. Y., et al. 2016, ApJS, 226, 20
Finke, J. D. 2013, ApJ, 763, 134
Foschini, L. 2011, RAA, 11, 1266
Foschini, L. 2017, FrASS, 4, 6
Foschini, L., Berton, M., Caccianiga, A., et al. 2015, A&A, 575, A13
Fossati, G., Maraschi, L., Celotti, A., Comastri, A., & Ghisellini, G. 1998, MNRAS, 299, 433
Ghisellini, G., Celotti, A., Fossati, G., Maraschi, L., & Comastri, A. 1998, MNRAS, 301, 451
Ghisellini, G., Righi, C., Costamante, L., & Tavecchio, F. 2017, MNRAS, 469, 255
Ghisellini, G., & Tavecchio, F. 2008, MNRAS, 387, 1669
Ghisellini, G., Tavecchio, F., Foschini, L., & Ghirlanda, G. 2011, MNRAS, 414, 2674
Giommi, P., Padovani, P., Polenta, G., et al. 2012, MNRAS, 420, 2899
Henri, G., & Saugé, L. 2006, ApJ, 640, 185
Kalita, N., Sawangwit, U., Gupta, A. C., & Wiita, P. J. 2019, ApJ, 880, 19
Kapanadze, B., Vercellone, S., & Romano, P. 2020, NewA, 79, 101393
Konopelko, A. K., Mastichiadis, A., Kirk, J. G., de Jager, O. C., & Stecker, F. W. 2003, ApJ, 597, 851
Krawczynski, H., Coppi, P. S., & Aharonian, F. 2001, ApJ, 559, 187
Mao, P., Urry, C. M., Massaro, F., et al. 2016, ApJS, 224, 26
Maraschi, L., Foschini, L., Ghisellini, G., Tavecchio, F., & Sambruna, R. M. 2008, MNRAS, 391, 1981
Maraschi, L., & Tavecchio, F. 2003, ApJ, 593, 667
Massaro, E., Perri, M., Giommi, P., & Nesci, R. 2004, A&A, 413, 489
Massaro, E., Tramacere, A., Perri, M., Giommi, P., & Tosti, G. 2006, A&A, 448, 861

Meyer, E. T., Fossati, G., Georganopoulos, M., & Lister, M. L. 2011, ApJ, 740, 98
Nieppola, E., Tornikoski, M., & Valtaoja, E. 2006, A&A, 445, 441
Nieppola, E., Valtaoja, E., Tornikoski, M., Hovatta, T., & Kotiranta, M. 2008, A&A, 488, 867
Oshlack, A. Y. K. N., Webster, R. L., & Whiting, M. T. 2001, ApJ, 558, 578
Padovani, P. 2007, Ap&SS, 309, 63
Padovani, P., Perlman, E. S., Landt, H., Giommi, P., & Perri, M. 2003, ApJ, 588, 128
Paggi, A., Cavaliere, A., Vittorini, V., & Tavani, M. 2009, A&A, 508, L31
Paliya, V. S., Ajello, M., Rakshit, S., et al. 2018, ApJL, 853, L2
Paliya, V. S., Parker, M. L., Jiang, J., et al. 2019, ApJ, 872, 169
Paliya, V. S., Stalin, C. S., Shukla, A., & Sahayanathan, S. 2013, ApJ, 768, 52
Piner, B. G., & Edwards, P. G. 2004, ApJ, 600, 115
Rakshit, S., Stalin, C. S., Chand, H., & Zhang, X. G. 2017, ApJS, 229, 39
Saugé, L., & Henri, G. 2004, ApJ, 616, 136
Sbarrato, T., Padovani, P., & Ghisellini, G. 2014, MNRAS, 445, 81
Sun, X. N., Zhang, J., Lin, D. B., et al. 2015, ApJ, 798, 43
Tavecchio, F., Maraschi, L., & Ghisellini, G. 1998, ApJ, 509, 608
Tramacere, A., Giommi, P., Perri, M., Verrecchia, F., & Tosti, G. 2009, A&A, 501, 879
Tramacere, A., Massaro, E., & Taylor, A. M. 2011, ApJ, 739, 66
Urry, C. M., & Padovani, P. 1995, PASA, 107, 803
Venters, T. M., Pavlidou, V., & Reyes, L. C. 2009, ApJ, 703, 1939
Xiong, D. R, Zhang, X., Bai, J. M., & Zhang, H. J. 2015, MNRAS, 451, 2750
Xue, R., Luo, D., Du, L. M., et al. 2016, MNRAS, 463, 3038
Yao, S., Yuan, W., Zhou, H., et al. 2015, MNRAS, 454, L16
Zhou, H., Wang, T., Yuan, W., et al. 2007, ApJL, 658, L13